

A bootstrap procedure for high-resolution velocity analysis

Mauricio D. Sacchi*

ABSTRACT

A method is given for further improving velocity estimates derived from high-resolution velocity analysis. In conventional velocity analysis, a set of tentative velocities is used to apply a normal moveout (NMO) correction to a set of spatio-temporal windows, the coherence measure is evaluated for each velocity and finally, the velocity estimate is retrieved from the peak of the coherence measure. Because analytical expressions for velocity uncertainties are difficult to derive, I propose an intensive statistical procedure, the bootstrap method, to assess the accuracy of the velocity estimate. In the bootstrap method, I create a data sample by randomly drawing seismic traces with replacement from a window of the common midpoint gather (CMP). Next, I calculate the velocity that maximizes the coherence measure for each bootstrap realization. The variation of this velocity provides a means to compute standard errors.

I also use the bootstrap method to construct an average coherence measure and a kernel density estimator of the velocity that maximizes the coherence. The average coherence exhibits an important attenuation of spurious events while retaining enough resolution to model reflections properly with similar moveout curves. The latter is illustrated with synthetic and field data examples.

vidual estimates of a given parameter may then be used to compute its standard errors and/or confidence intervals. In seismology, bootstrap methods have been applied to different problems: estimation of earthquake magnitude uncertainties (McLaughlin, 1988), estimation of standard error of earthquake depths (Tichelaar and Ruff, 1989), estimation of shear-wave splitting errors (Sandvol and Hearn, 1994), and velocity and depth errors determined by stacking receiver functions (Gurrola et al., 1994). The bootstrap scheme was also applied by Tauxe et al. (1991) to analyze directional paleomagnetic data. In time series analysis, Sacchi and Ulrych (1994) use the Extended Information Criterion, which is based on the bootstrap method, to estimate optimum trade-off parameters in seismic deconvolution. This criterion was also used to estimate the number of harmonics required to model a deterministic time series (Ulrych and Sacchi, 1995).

Velocity analysis, in general, is based on the identification of the peaks of a coherence measure. A set of trial velocities is used to apply on normal moveout (NMO) correction to a window in the common midpoint (CMP) gather; the velocity estimate is that velocity which maximizes the coherence measure (Neidell and Taner, 1971). In this problem the statistic of interest is the velocity where the coherence measure exhibits a peak.

In this paper, the coherence measure is derived from the eigenspectra of the covariance matrix of the data (Key and Smithson, 1990). The bootstrap technique is used to retrieve velocity peaks with the associated standard errors, an average coherence measure, and a Gaussian kernel density estimate (Silverman, 1986) of the velocity that maximizes the coherence.

INTRODUCTION

The bootstrap procedure (Appendix A), originally developed by Efron (1979) to compute standard errors, is a computer-intensive technique for assigning measures of accuracy to statistical estimates. The technique can be also used to assign confidence intervals (Efron and Tibshirani, 1993). In general, bootstrap methods are well suited for problems where the parameters of interest cannot be estimated by analytical means.

The basic idea in bootstrapping is that the actual data are resampled to produce a large number of data sets. The indi-

VELOCITY ANALYSIS

In a CMP gather the moveout curve of a reflection is generally approximated by

$$t_i = (t_0^2 + d_i^2/v^2)^{1/2} \quad i = 1, 2, \dots, N, \quad (1)$$

where d_i is the source-receiver offset at the i th trace, v is the velocity of the reflection, and t_0 is the two-way zero-offset traveltime. The velocity analysis is performed in consecutive temporal windows by evaluating a coherence measure along the

Manuscript received by the Editor July 22, 1996; revised manuscript received March 10, 1998.

*Department of Physics, University of Alberta, Abadh Bhatia Physics Laboratory, Edmonton, AB T6G 2J1, Canada; E-mail: sacchi@phys.ualberta.ca.

© 1998 Society of Exploration Geophysicists. All rights reserved.

List of symbols

B	= Number of bootstrap realizations
$C(t_0, v)$	= Coherence measure at intercept time t_0 and velocity v
$C_i^*(t_0, v)$	= Coherence measure derived from the resampled data, $i = 1, B$
$\langle C^*(t_0, v) \rangle$	= Mean coherence obtained via equation (6)
$\mathbf{R}(t_0, v)$	= Data covariance matrix
$\hat{\mathbf{R}}(t_0, v)$	= Estimator of the data covariance matrix
$\hat{\mathbf{R}}_i^*(t_0, v)$	= Estimator of the data covariance matrix computed from the resampled data
\mathbf{R}_s	= Signal covariance matrix
σ_n^2	= Variance of the uncorrelated noise
$\mathbf{X}(t_0, v)$	= Data matrix; each row corresponds to a segment of $2M + 1$ samples of a seismic trace centered about a moveout curve with intercept time t_0 and velocity v
$\mathbf{X}_i^*(t_0, v)$	= Data matrix after resampling with replacement the rows of $\mathbf{X}(t_0, v)$
$v_i^*(t_0)$	= Velocity that maximizes the coherence $C(t_0, v)_i^*$, $i = 1, B$
$\langle v^*(t_0) \rangle$	= Mean velocity after B bootstrap realizations [equation (4)]
$\sigma^*(t_0)$	= Standard error of the velocity estimate at intercept time t_0 computed after B bootstrap realizations [equation (5)]
λ_i	= Eigenvalues of the covariance matrix
$\hat{\lambda}_i$	= Eigenvalues of the estimator of the covariance matrix

moveout curve. The analysis is carried out for a set of trial velocities; the velocity corresponding to the peak of the coherence measure is interpreted as the velocity that best flattens the seismic event. However, finite aperture, additive noise, static shifts, and departures from the hyperbolic model may deteriorate the accuracy of the estimate.

If $C(t_0, v)$ denotes a coherence measure of interest at a window centered at $t = t_0$, an estimate of the velocity v is obtained at the peak value of $C(t_0, v)$.

Bootstrap application

The coherence measure described in Appendix B, $C(t_0, v)$, depends on the eigenvalues of the data covariance matrix. The data window of length $2M + 1$ centered about a moveout curve with intercept time, t_0 , and velocity, v , is expressed as follows:

$$\mathbf{X}(t_0, v) = \begin{pmatrix} x_{1,t_0-M\Delta t} & \cdots & x_{1,t_0} & \cdots & x_{1,t_0+M\Delta t} \\ x_{2,t_0-M\Delta t} & \cdots & x_{2,t_0} & \cdots & x_{2,t_0+M\Delta t} \\ x_{3,t_0-M\Delta t} & \cdots & x_{3,t_0} & \cdots & x_{3,t_0+M\Delta t} \\ \cdots & \cdots & \cdots & \cdots & \cdots \\ x_{N,t_0-M\Delta t} & \cdots & x_{N,t_0} & \cdots & x_{N,t_0+M\Delta t} \end{pmatrix}, \quad (2)$$

where $x_{j,t_0+k\Delta t}$ indicates the amplitude of trace j at the interpolated time sample $t_0 + k\Delta t$. The estimate of the data covariance

matrix from equation (B-8) becomes

$$\hat{\mathbf{R}}(t_0, v) = \frac{1}{2M + 1} \mathbf{X}(t_0, v) \mathbf{X}^T(t_0, v). \quad (3)$$

In the bootstrap procedure, B coherence measures $C_i^*(t_0, v)$, $i = 1, B$ are computed by sampling with replacement the rows or the matrix $\mathbf{X}(t_0, v)$. The resampled data window at the bootstrap realization i is denoted by $\mathbf{X}_i^*(t_0, v)$. This is used to compute the i th realization of the data covariance matrix $\hat{\mathbf{R}}_i^*(t_0, v)$ and its associated coherence measure $C_i^*(t_0, v)$. From the maxima of each coherence measure, I estimate B bootstrap estimates of the velocity $v^*(t_0)_1, v^*(t_0)_2, \dots, v^*(t_0)_B$. This set of velocities is used to obtain a mean velocity and its standard deviation,

$$\langle v^*(t_0) \rangle = \frac{1}{B} \sum_{i=1}^B v_i^*(t_0) \quad (4)$$

and

$$\sigma^*(t_0) = \sqrt{\frac{1}{B-1} \sum_{i=1}^B [v_i^*(t_0) - \langle v^*(t_0) \rangle]^2}. \quad (5)$$

The bootstrap technique is also used to compute a mean coherence measure,

$$\langle C^*(t_0, v) \rangle = \frac{1}{B} \sum_{i=1}^B C_i^*(t_0, v). \quad (6)$$

Later examples show that the mean coherence measure drastically reduces spurious maxima that may lead to misleading interpretations.

Figure 1 is the data window for a single reflection after applying an NMO correction with an incorrect velocity. In the same panel I reproduce two bootstrap realizations obtained by resampling with replacement the traces of the data window [rows of $\mathbf{X}(t_0, v)$]. Figure 2 shows the reflection after NMO

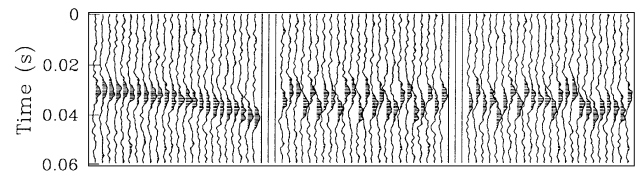


FIG. 1. A reflection within a gate of analysis after NMO correction. An incorrect velocity, v , was used to perform the NMO correction (left). The left panel is mathematically represented in the text with the matrix $\mathbf{X}(t_0, v)$, where t_0 is the intercept time associated to the center of the gate and v is the velocity used to perform the NMO correction. Two bootstrap realizations (center and right), $\mathbf{X}_i^*(t_0, v)$, were computed by resampling with replacement traces from the original window (left).

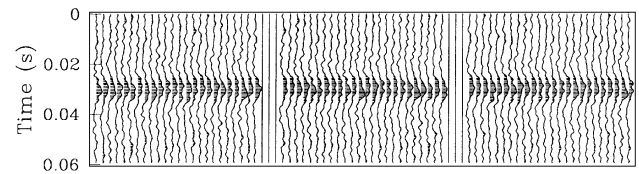


FIG. 2. A reflection within a gate of analysis after NMO correction. The correct velocity, v , was used to perform the NMO correction (left). Two bootstrap realizations (center and right) were computed from the original window (left).

correction with the correct velocity together with two bootstrap realizations. When the right velocity is used, the coherence of the signal is not affected. An accurate velocity will flatten the coherent reflector. Hence, interchanging traces [rows of $\mathbf{X}(t_0, v)$] will only alter the influence of the noise in the structure of the covariance matrix $\mathbf{R}(t_0, v)$. When the trial velocity does not accurately predict the moveout of the reflection, the bootstrap procedure will help to minimize near-offset contributions that tend to broaden the coherence peak.

The output of the bootstrap procedure is a table of mean velocities and standard errors for each temporal window which may be used for automatic event detection. In this case, the presence or absence of signal may be assessed by a simple test on the standard error of the velocity. Only velocities with standard error below a given threshold are considered to indicate signal.

According to Efron and Tibshirani (1993), $B = 50$ is often enough to give a good estimate of standard errors. In contrast, the number of bootstrap samples needs to be much larger to compute confidence intervals ($B > 1000$), thereby requiring a significant computational effort. However, a target-oriented analysis may substantially decrease the computational cost by limiting the temporal analysis windows in the CMP to fall within the zone of interest. Partial stacking (summation of adjacent traces after correction) may improve the estimation of the data covariance matrix. Another advantage of partial stacking is the reduction of the dimension of the covariance matrix and therefore also the computational cost of the procedure (Biondi and Kostov, 1989).

EXAMPLES

Synthetic simulation

The CMP in Figure 3 consists of 36 traces distributed between 40 and 1400 m in 40-m increments. Two reflections of 2400 and 2500 m/s located at $t_0 = 0.4$ s were used to test the resolution of this algorithm. Two single reflections were simulated at 0.6 and 0.8 s (Table 1).

The coherence measure was retrieved from the original 36 traces using 16 gates of length 0.06 s or $M = \pm 8$ samples. The data covariance matrix is computed using equation (3)

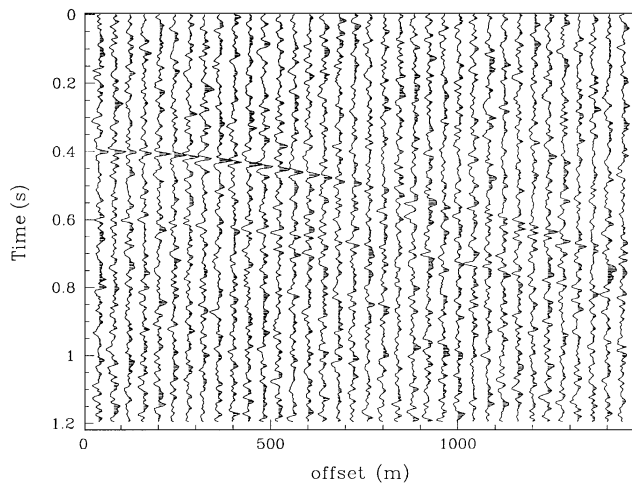


FIG. 3. A synthetic CMP. The data were computed from the parameters shown in Table 2.

after a partial stacking of 6 nonoverlapping adjacent traces. This operation leads to a 6×6 covariance matrix and a partial improvement of the S/N ratio. At this point some comments are in order. First, it is clear that the doublet has not been properly resolved by the coherence measure. In fact, at $t = 0.4$ s we can visualize three peaks. Second, the relative amplitude of the peaks is not modeled correctly. Figure 5 shows the coherence at four different values of the intercept time, $t_0 = 0.2, 0.4, 0.6,$ and 0.8 s.

The average coherence measure computed after 50 bootstrap realizations is portrayed in Figures 6 and 7. In this case, the doublet is properly resolved and the relative amplitude of the peaks is honored.

The reason the coherence computed from the data itself (without random replacement) cannot identify the presence of the doublet at 0.4 s is a direct consequence of a measure devised to identify a single event (Key and Smithson, 1990). The false peak located between the true velocities (2400 and 2500 m/s) in Figure 4 is because of a coherent alignment of near-offset energy from both reflections. Since the average coherence (Figure 7) can identify the doublet correctly, it appears that the bootstrap procedure annihilates any coherent alignment of energy at the intermediate velocity. The latter has a simple explanation: when one of the reflections is flattened properly, the random replacement of traces destroys any residual coherence provoked by the presence of multiple waveforms. In the long run, the average coherence clearly enhances the two peaks (Figures 6 and 7).

The Gaussian density kernel estimator (Appendix C) of the velocity is displayed in Figures 8 and 9. The vertical bars in Figure 9 indicate the position of the mean velocity and the standard errors. The density estimator exhibits a clear bimodal behavior at 0.4 s. The mean corresponds to the mean of the population. In this case the peak of the density provides an estimate of the velocity. For a unimodal and approximately symmetric distribution, we can always identify the peak with the mean. It is interesting to analyze the coherence measure at $t_0 = 0.2$ s. In this case, the density estimator resembles a uniform distribution. In other words, in the absence of signal, any velocity can maximize the coherence. The bootstrap velocities are shown in Table 2. Note that the variance of the velocity is much larger where the density is wider (Figures 8 and 9) and has several maxima (multiple events).

Field data example

An ensemble of 10 consecutive land CMP gathers (Figure 10) was used to test the algorithm. The minimum offset is 50 m, and the maximum offset is 1900 m. The corresponding semblance panel is shown in Figure 11. The high-resolution analysis is used to identify short-period multiple interferences.

Table 1. Synthetic CMP gather.

Event	t [s]*	v [m/s] [‡]	A^{**}
1	0.4	2400	1.0
2	0.4	2500	0.8
3	0.6	2500	-1.0
4	0.8	2600	0.5

*Two-way travelttime.

‡Velocity.

**Peak amplitude of wavelet.

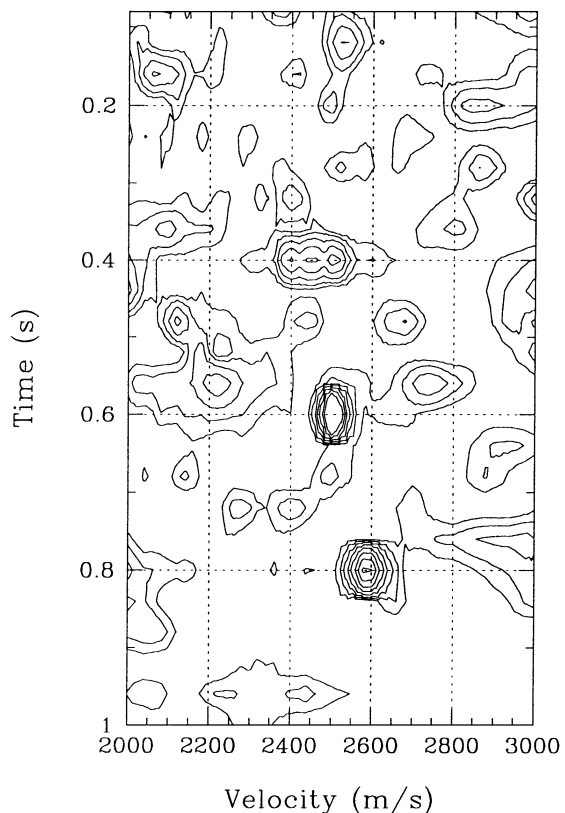


FIG. 4. The velocity spectrum shown at $t_0 = 0.2, 0.4, 0.6,$ and 0.8 s (Figure 3). The coherence does not properly resolve the reflections at 0.4 s.

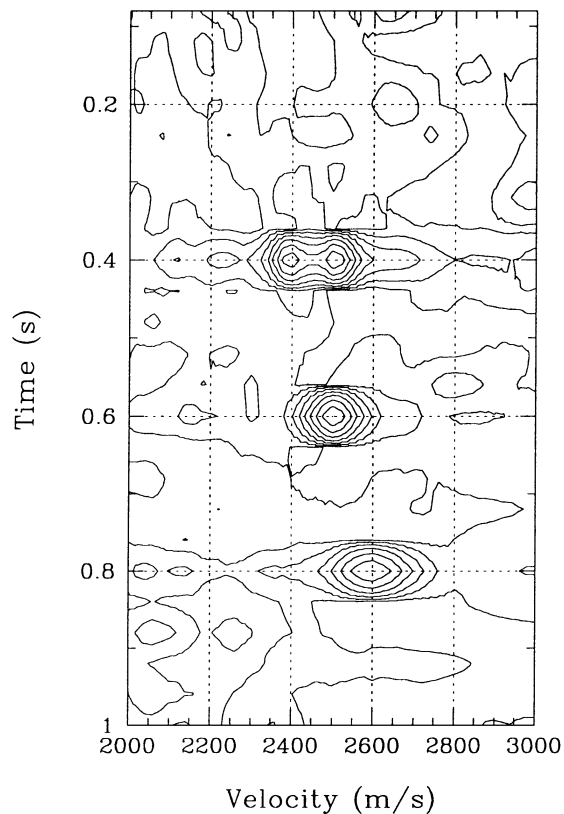


FIG. 6. The mean coherence measure derived after 50 bootstrap realizations. Time slices of velocity spectrum at $t_0 = 0.2, 0.4, 0.6,$ and 0.8 s (Figure 4). The coherence reflections at 0.4 s are clearly distinguished. True velocities at $t_0 = 0.4$ s are $v = 2400$ and 2500 m/s.

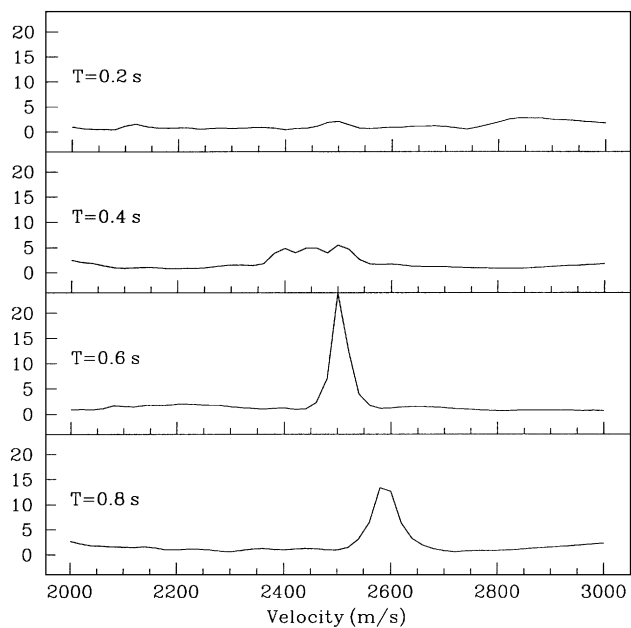


FIG. 5. The mean coherence measure computed after 50 bootstrap replications.

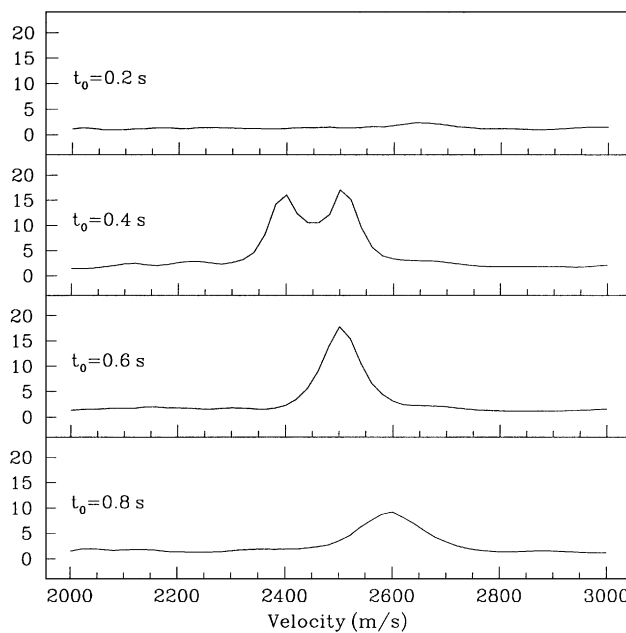


FIG. 7. The coherence measure computed from the synthetic CMP shown in Figure 2.

Table 2. Synthetic example. The true reflections are located at $t = 0.4, 0.6,$ and 0.8 s (gates 9, 14, 19). Note the drop in the standard error in those gates.

Gate	t [s]*	v [m/s]‡	σ **	$v + 2\sigma$	$v - 2\sigma$
1	0.08	2360	253	2867	1852
2	0.12	2351	295	2941	1761
3	0.16	2426	296	3019	1832
4	0.20	2503	248	2999	2006
5	0.24	2482	309	3100	1863
6	0.28	2466	251	2969	1963
7	0.32	2540	329	3199	1880
8	0.36	2439	223	2885	1993
9	0.40	2464	52	2568	2359
10	0.44	2394	280	2954	1833
11	0.48	2282	237	2757	1806
12	0.52	2397	314	3026	1767
13	0.56	2440	276	2993	1888
14	0.60	2502	14	2531	2473
15	0.64	2543	298	3139	1946
16	0.68	2466	362	3190	1741
17	0.72	2423	321	3066	1780
18	0.76	2540	329	3199	1880
19	0.80	2594	21	2636	2552
20	0.84	2452	352	3158	1747
21	0.88	2276	277	2831	1721
22	0.92	2455	276	3008	1902
23	0.96	2315	263	2842	1787
24	1.00	2492	296	3084	1900

*Two-way traveltime.

‡Mean velocity after 50 bootstrap replications.

**Sample standard deviation.

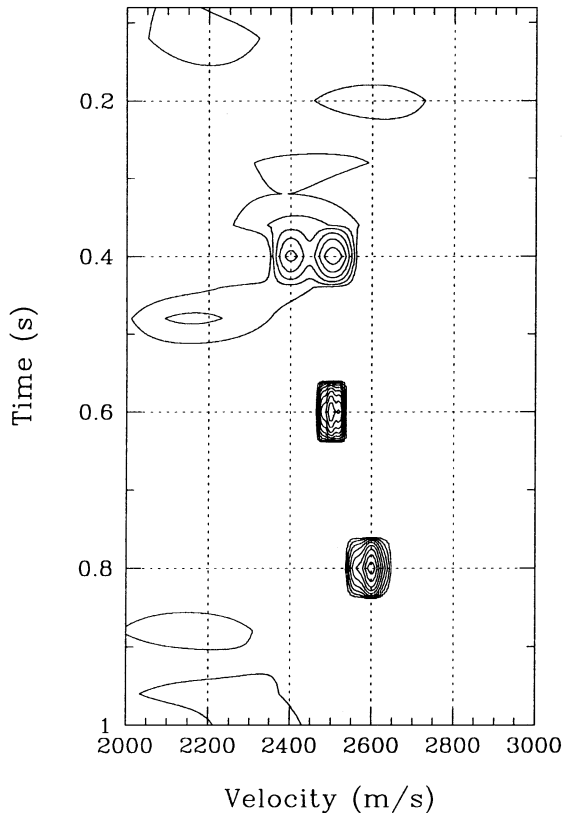


FIG. 8. The Gaussian density estimator of the velocity that maximizes the coherence measure.

The high-resolution coherence measure is displayed in Figure 12. Although the resolution is enhanced, several ill-defined minima may represent seismic events. The mean coherence measure computed after 100 bootstrap samples is displayed in Figure 13. Now the main features of the velocity panel are discernible. The multiple interferences are visible at $t_0 \approx 1.05$ s and $t_0 \approx 1.15$ s. The Gaussian density kernel estimate of the velocity peaks (Figure 14) presents a clear picture of the velocity spectrum. The multiples are located at $t_0 \approx 1.05, 1.12, 1.15,$ and 1.2 s. Table 4 shows the bootstrapped velocities and the standard errors. The presence of multiple events increases the standard error of the velocity (gate 17 in Table 3).

DISCUSSION AND CONCLUSION

The bootstrap procedure may be used to assign errors to seismic velocities and to improve the velocity spectrum computed from high-resolution coherence measures. The computational cost of the problem may appear too excessive because the individual cost of an already high-velocity analysis technique is multiplied by the number of bootstrap realizations. However, the procedure can be accelerated by partial stacking and/or target-oriented processing.

In the presence of multiples, the bootstrap procedure helps annihilate spurious peaks that may result in a misleading interpretation of the velocity spectrum. The standard deviation of the velocity estimate can be computed; it is important to stress, however, that the variance estimate may be an indicator of multiple maxima in the velocity panel. The mean velocity and its standard deviation can be used to estimate accuracy

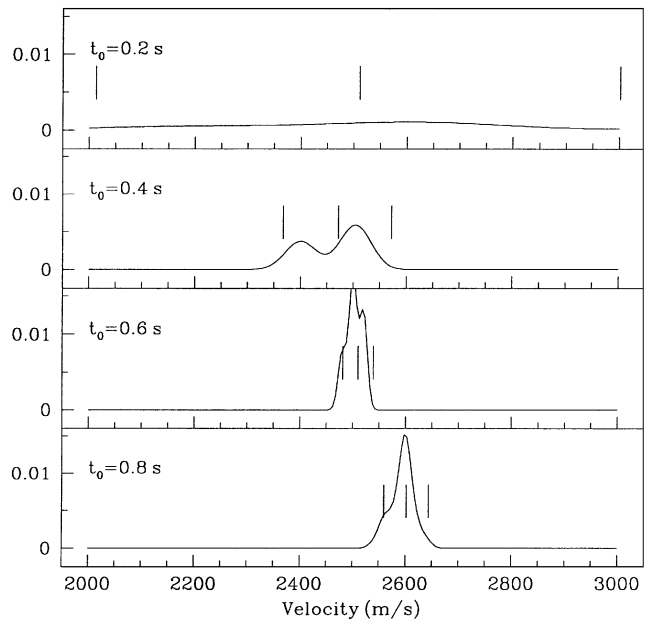


FIG. 9. Time slices of the Gaussian density kernel estimator of the velocity that maximizes the coherence measure (Figure 8). Vertical bars indicate the position of the mean velocity and the $\pm 2\sigma$ bounds. In the upper part of the diagram (0.2 s), the bootstrap analysis captures the flat signature that resembles a uniform probability. In the absence of signal, the velocity spectrum can exhibit a peak anywhere (no preferable velocity). The bimodality at $t_0 = 0.4$ s reflects the presence of the doublet.

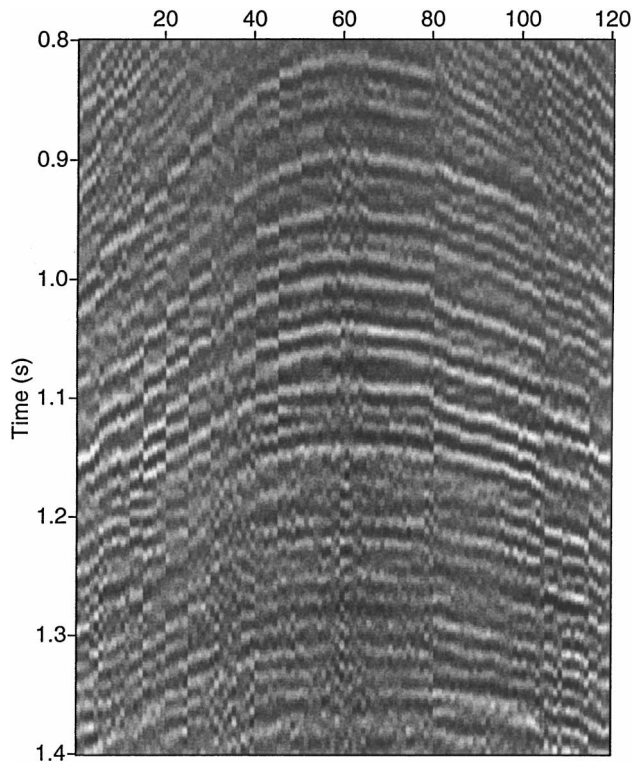


FIG. 10. Ensemble of 10 adjacent CMP gathers forming a super CMP gather used for velocity analysis.

only when the assumption of a single waveform within the gate of analysis is valid. In a general scenario, the Gaussian density kernel estimator of the velocity offers an alternative manner to interpret velocity panels. The Gaussian kernel density estimate of the velocity gives an idea of how many times a velocity maximizes the coherence during the bootstrap simulation.

ACKNOWLEDGMENTS

This work was supported by the CDSST at UBC. Real data have been graciously provided by PanCanadian Petroleum Ltd. I thank Drs. T. Ulrych and M. Bostock for many helpful discussions and suggestions. Comments and suggestions of Kurt Marfurt and an anonymous reviewer have improved the final form of the manuscript.

REFERENCES

Bendat, J. S., and Piersol, A. G., 1971, Random data: Analysis and measurement procedures: Wiley-Interscience.
 Bienvenu, G., and Kopp, L., 1983, Optimality of high resolution array processing using the eigensystem approach: IEEE Trans. Acoust., Speech, Signal Processing, **ASSP-31**, 1235-1248.
 Biondi, B. L., and Kostov, C., 1989, High-resolution velocity spectra using eigenstructure methods: Geophysics, **54**, 832-842.
 Efron, B., 1979, Bootstrap methods: Another look at the jackknife: Ann. Statist., **7**, 1-26.
 Efron, B., and Tibshirani, R., 1993, An introduction to the bootstrap method: Chapman and Hall.
 Gurrola, H., Minster, J. B., and Owens, T., 1994, The use of velocity spectrum for stacking receiver functions and imaging upper mantle discontinuities: Geophys. J. Int., **117**, 427-440.
 Key, S. C., and Smithson, S. B., 1990, New approach to seismic-event detection and velocity determination: Geophysics, **55**, 1057-1069.

Table 3. Field data. The standard error is much larger when the density peaks are wider or when the density panel has several maxima that reflect the presence of multiples (see Figure 13).

Gate	t [s]*	v [m/s]‡	σ **	$v + 2\sigma$	$v - 2\sigma$
1	0.800	3168	64	3232	3103
2	0.814	3155	63	3218	3092
3	0.828	3139	42	3182	3097
4	0.842	3132	109	3242	3023
5	0.856	3139	41	3180	3098
6	0.870	3149	59	3208	3090
7	0.884	3189	41	3230	3148
8	0.898	3193	52	3245	3141
9	0.912	3191	88	3279	3103
10	0.926	3168	63	3232	3104
11	0.940	3191	47	3239	3144
12	0.954	3190	45	3236	3144
13	0.968	3225	61	3287	3164
14	0.982	3239	41	3280	3198
15	0.996	3239	41	3280	3198
16	1.010	3237	48	3285	3188
17	1.024	3255	276	3531	2978
18	1.038	3376	59	3436	3317
19	1.052	3336	59	3396	3276
20	1.066	3346	53	3399	3292
21	1.080	3475	64	3540	3411
22	1.094	3524	61	3585	3462
23	1.108	3446	356	3803	3089
24	1.122	3306	443	3750	2863
25	1.136	3460	285	3745	3174
26	1.150	3368	644	4012	2723
27	1.164	3328	170	3498	3157
28	1.178	3284	248	3533	3035
29	1.192	3304	204	3508	3100
30	1.206	3074	342	3417	2732
31	1.220	3558	665	4223	2892
32	1.234	3533	202	3736	3331
33	1.248	3759	189	3948	3570
34	1.262	3820	132	3952	3687
35	1.276	3833	451	4285	3381
36	1.290	3950	62	4012	3888
37	1.304	3982	62	4045	3919
38	1.318	3987	406	4393	3580
39	1.332	3757	1315	5072	2441
40	1.346	3608	840	4448	2768

*Two-way traveltime.

‡Mean velocity after 100 bootstrap replications.

**Sample standard deviation.

Kirlin, R. L., 1992, The relationship between the semblance and the eigenstructure velocity estimators: Geophysics, **57**, 1027-1033.
 McLaughlin, K. L., 1988, Maximum-likelihood event magnitude estimation with bootstrapping for uncertainty estimation: Bull., Seis. Soc. Am., **78**, 855-862.
 Neidell, N. S., and Taner, M. T., 1971, Semblance and other coherency measures for multichannel data: Geophysics, **34**, 482-497.
 Sacchi, M. D., and Ulrych, T. J., 1994, Estimation of optimum tradeoff parameters using a new information criterion: An application to deconvolution: J. Seis. Expl., **3**, 261-272.
 Sandvol, E., and Hearn, T., 1994, Bootstrapping shear-wave splitting errors: Bull. Seis. Soc. Am., **84**, 1971-1977.
 Silverman, B. W., 1986, Density estimation for statistics and data analysis: Chapman and Hall.
 Tauxe, L., Kylstra, N., and Constable, C., 1991, Bootstrap statistic for paleomagnetic data: J. Geophys. Res., **96**, 11 723-11 740.
 Tichelaar, B. W., and Ruff, L. J., 1989, How good are our best models?: EOS Trans. Am. Geophys. Union, **68**, 659-606.
 Ulrych, T. J., and Sacchi, M. D., 1995, Sompi, Pisarenko and the extended information criterion: Geophys. J. Internat., **122**, 719-724.
 Wax, M., Shan, T., and Kailath, T., 1984, Spatio-temporal spectral analysis by eigenstructure methods: IEEE Trans. Acoust., Speech, Signal Processing, **ASSP-32**, 817-827.

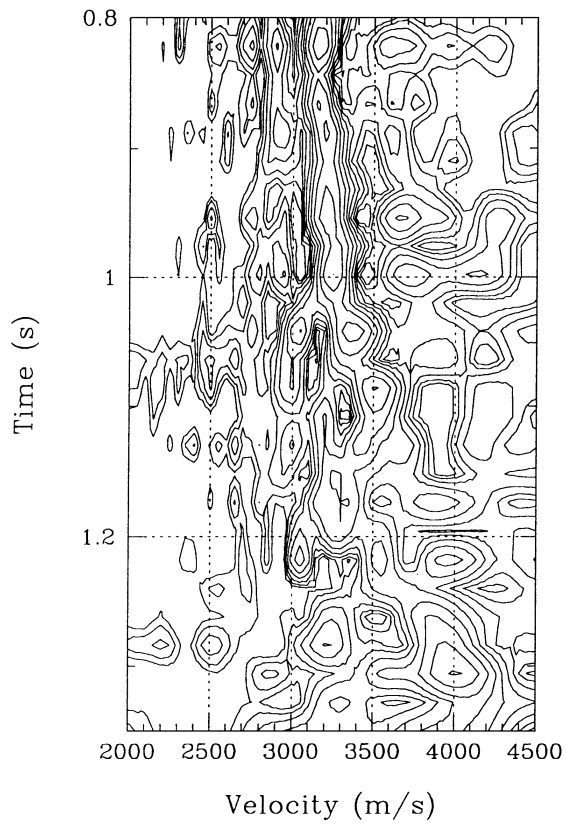


FIG. 11. Conventional semblance analysis of the super CMP gather shown in Figure 10.

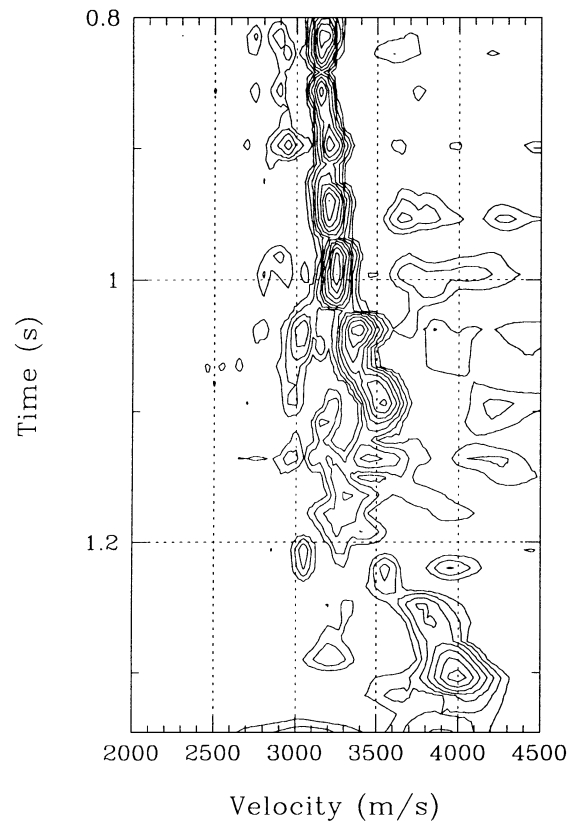


FIG. 13. Mean coherence measure calculated using 100 bootstrap realizations.

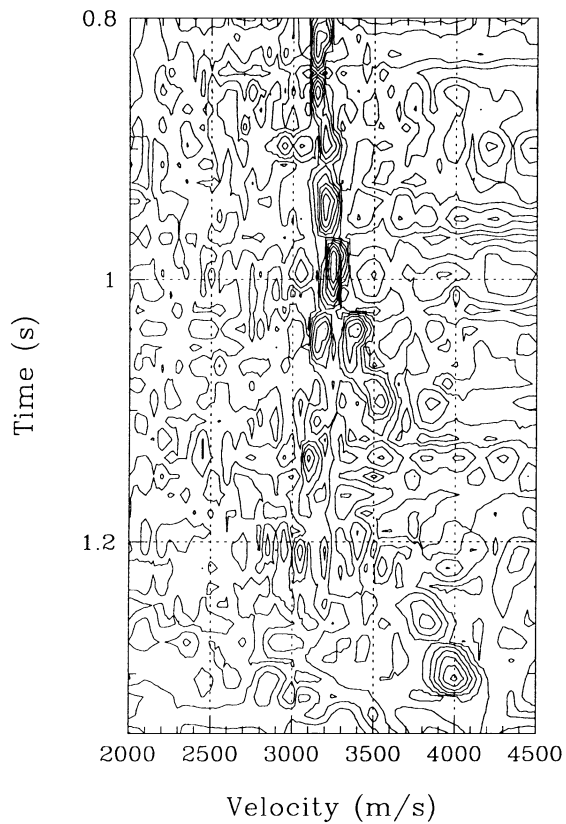


FIG. 12. Coherence measure computed from the super CMP.

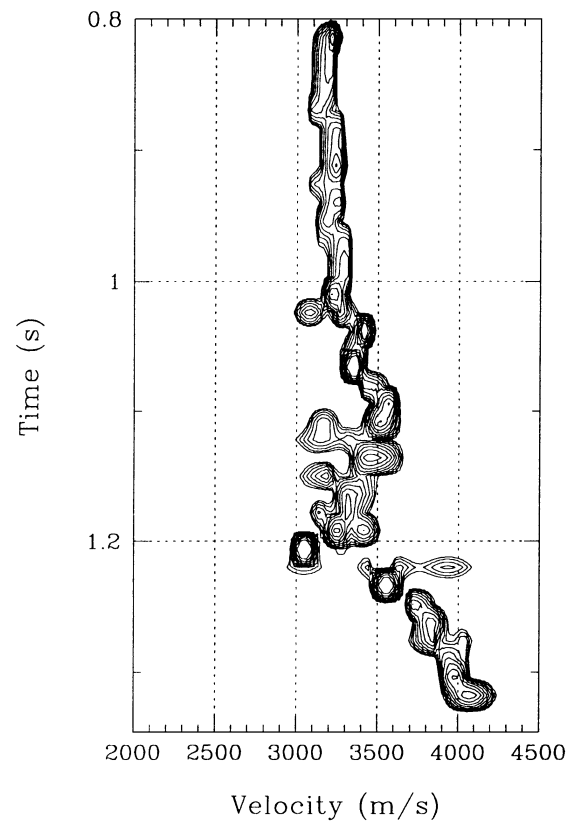


FIG. 14. Gaussian kernel density estimator of the velocity peaks.

APPENDIX A
THE BOOTSTRAP METHOD

Suppose we have observed N samples of a generic variable $\mathbf{x} = (x_1, x_2, x_3, \dots, x_N)$, from which we compute a statistic of interest, $S(\mathbf{x})$. A bootstrap sample, $\mathbf{x}^* = (x_1^*, x_2^*, x_3^*, \dots, x_N^*)$, is obtained by randomly sampling the original data with replacement

$$x_i^* = x_k, \quad i = 1, \dots, N, \quad (\text{A-1})$$

where k is a random uniform variable that can take values $1, 2, 3, \dots, N$. The data may be numbers, vectors, matrices, or any other structure, depending on the problem (Efron and Tibshirani, 1993).

The bootstrap procedure to compute the standard error of the statistic, $S(\mathbf{x})$, is summarized as follows:

- 1) Compute B bootstrap samples, $\mathbf{x}_1^*, \mathbf{x}_2^*, \mathbf{x}_3^*, \dots, \mathbf{x}_B^*$, each consisting of N values drawn with replacement from \mathbf{x} .

- 2) Evaluate the statistic of interest associated with each bootstrap sample

$$\hat{\theta}_i^* = S(\mathbf{x}_i^*), \quad i = 1, 2, \dots, B. \quad (\text{A-2})$$

- 3) Estimate the standard deviation using the expression

$$\sigma^* = \left[\frac{1}{B-1} \sum_{i=1}^B (\theta_i^* - \langle \theta^* \rangle)^2 \right]^{1/2}, \quad (\text{A-3})$$

where $\langle \theta^* \rangle = \sum_{i=1}^B \theta_i^* / B$.

The statistic $S(\mathbf{x})$ may not have an analytical form. Moreover, it may be obtained as a cascade of different numerical procedures. Figure A-1 illustrates the bootstrap procedure for determining standard errors. The individual estimators $\theta_i^*, i = 1, B$ can be used to compute other statistics, i.e., confidence intervals, a histogram of θ , or a Gaussian kernel density estimator, which is a smooth representation of the histogram (Appendix C).

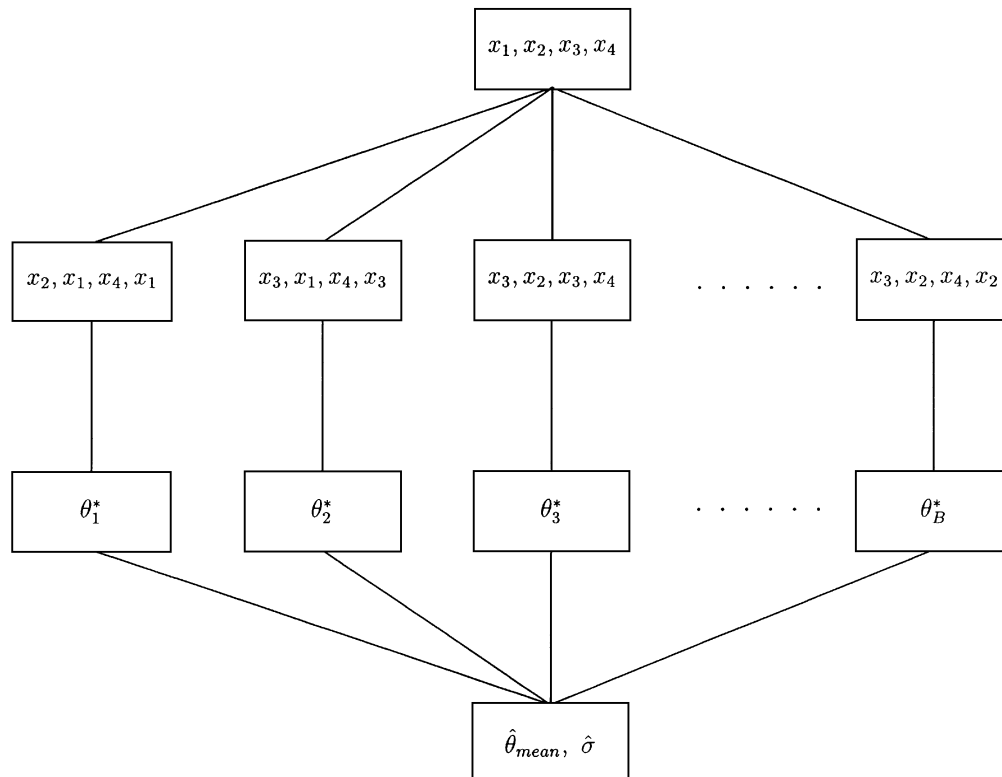


FIG. A-1. Schematic representation of the bootstrap method. The original data (x_1, x_2, x_3, x_4) are resampled by randomly selecting four elements with replacement. This is repeated B times to form the bootstrap estimate, $\theta_i^*, i = 1, B$. The B estimates are used to compute the mean and the variance.

APPENDIX B
COHERENCE MEASURES

The coherence measure of interest is derived from the eigen-spectra of the covariance matrix of the data. Techniques that exploit the eigenstructure of the covariance matrix have been borrowed from the field of array processing (Bienvenu and Kopp, 1983; Wax et al., 1984) and applied to velocity analysis by different researchers (Biondi and Kostov, 1989; Key and Smithson, 1990; Kirilin, 1992).

The seismic signal, in the presence of noise, at receiver i may be modeled using the equation

$$x_i(t) = s(t - \tau_i) + n_i(t) \quad i = 1, N, \quad (\text{B-1})$$

where $\tau_i = (t_0^2 + d_i^2/v^2)^{1/2} - t_0$ is the delay of the signal between the i th receiver and a receiver having $d_0 = 0$. If a waveform is extracted along a hyperbolic path parameterized with velocity v , equation (B-1) may be rewritten as

$$x_i(t) = s(t) + n_i(t) \quad i = 1, N, \quad (\text{B-2})$$

where, to avoid notational clutter, I use the same variable $x(t)$ to designate the delayed waveform [equation (B-1)] and the corrected waveform [equation (B-2)]. The covariance matrix of the signal is defined as

$$R_{i,j}(t) = E[x_i(t)x_j(t)] \quad i, j = 1, N, \quad (\text{B-3})$$

where E denotes the expectation operator. If we assume the noise and signal to be uncorrelated, the data covariance matrix becomes

$$R_{i,j}(t) = R_{si,j}(t) + \sigma_n^2(t)\delta_{i,j}, \quad (\text{B-4})$$

where $R_{si,j}(t)$ denotes the signal covariance matrix and $\delta_{i,j} = 1$ if $i = j$ and $\delta_{i,j} = 0$ otherwise.

Assuming a stationary source and a stationary noise process, we may drop the dependence on t . It is easy to verify that the eigenvalues of the covariance matrix become

$$\lambda_i = \lambda_{si} + \sigma_n^2 \quad i = 1, 2, \dots, N, \quad (\text{B-5})$$

where λ_{si} are the eigenvalues of the signal covariance matrix. Assuming the signal is invariant across each trace, the signal covariance matrix is rank one, and we can write the following relationships:

$$\lambda_{s1} = N \cdot P_s \quad (\text{B-6})$$

$$\lambda_{si} = 0 \quad i = 2, \dots, N,$$

where $P_s = E[s(t)^2]$ denotes the signal power. Using equation (B-5), the eigenvalues of the data covariance matrix become

$$\lambda_1 = N \cdot P_s + \sigma_n^2 \quad (\text{B-7})$$

$$\lambda_i = \sigma_n^2 \quad i = 2, \dots, N.$$

For uncorrelated noise, the minimal $N - 1$ eigenvalues of the data are equal to the variance of the noise. The largest eigenvalue is proportional to the power of energy of the coherent signal plus the variance of the noise.

In real situations, the eigenspectrum is retrieved from an estimate of the data covariance matrix. If the stationary random processes $x_i(t)$ and $x_j(t)$ are ergodic, the ensemble averages defined in equation (B-3) can be replaced by time averages (see, for instance, Bendat and Piersol, 1971). The estimator of the covariance matrix becomes

$$\hat{R}_{i,j} = \frac{1}{2M+1} \sum_{k=-M}^M x_i(k\Delta t)x_j(k\Delta t). \quad (\text{B-8})$$

Using the results given in equations (B-6) and (B-7), it is evident that an estimator of the noise variance is

$$\hat{\sigma}_n^2 = \frac{1}{N-1} \sum_{i=2}^N \hat{\lambda}_i. \quad (\text{B-9})$$

Similarly, an estimator of the signal energy is given by

$$\hat{P}_s = \frac{\hat{\lambda}_1 - \hat{\sigma}_n^2}{N}, \quad (\text{B-10})$$

and equations (B-9) and (B-10) can be combined into a single measure, the S/N ratio:

$$\hat{C} = \frac{1}{N} \frac{\hat{\lambda}_1 - \sum_{i=2}^N \hat{\lambda}_i / (N-1)}{\sum_{i=2}^N \hat{\lambda}_i / (N-1)}. \quad (\text{B-11})$$

The coherence measure, \hat{C} , was devised assuming the presence of a signal and assuming the proper velocity is used to extract the waveform. In general \hat{C} is computed for different gates and different trial velocities. It is convenient to implicitly emphasize the dependence of the coherence on these parameters by denoting $\hat{C}(t_0, v)$. When the gate of analysis contains only noise, $\hat{C}(t_0, v)$ tends toward zero. When the trial velocity does not match the velocity of the reflection, it is impossible to decompose the eigenstructure of the data into signal and noise contributions. In this case, the covariance matrix has a complete set of eigenvalues different from zero; therefore, it is not possible to recognize which part of the eigenspectrum belongs to the noise and which belongs to the signal process.

Key and Smithson (1990) propose another coherence measure based on a log-generalized likelihood ratio that tests the hypothesis of equality of eigenvalues:

$$\hat{W}_{ml} = M \log^N \left[\frac{(\sum_{i=1}^N \hat{\lambda}_i / N)^N}{\prod_{i=1}^N \hat{\lambda}_i} \right]. \quad (\text{B-12})$$

In the absence of signal, $\lambda_i = \sigma_n^2$, $i = 1, N$ and hence $W_{ml} = 0$. In the presence of a single reflected signal, $\lambda_1 \neq 0$, $\lambda_i = 0$, $i = 2, N$ and $W_{ml} \rightarrow \infty$. Therefore, W_{ml} provides a strong discrimination between signal and noise. Key and Smithson (1990) combine equations (B-11) and (B-12) into a single measure, K_{ml} , given

by the product

$$\hat{K}_{ml} = \hat{W}_{ml} \hat{C}. \tag{B-13}$$

Only one eigenvalue, λ_1 , is required to estimate \hat{C} , since

$$\text{trace}(\hat{\mathbf{R}}) = \hat{\lambda}_1 + \hat{\lambda}_2 + \dots + \hat{\lambda}_N, \tag{B-14}$$

where

$$\text{trace}(\hat{\mathbf{R}}) = \sum_{i=1}^N \hat{R}_{ii}. \tag{B-15}$$

It is easy to see from equations (B-11) and (B-14) that only $\hat{\lambda}_1$ is needed to compute \hat{C} .

APPENDIX C

THE GAUSSIAN DENSITY KERNEL ESTIMATOR

The set of velocities $v_b^*(t_0)$, $b = 1, B$ may be also used to compute the velocity histogram at t_0 . It is difficult, however, to display a suite of histograms in a single velocity panel. To obtain a smoother representation of the histogram, I use a Gaussian kernel density estimate (Silverman, 1986). The Gaussian density estimate is computed using the following expression:

$$\hat{f}(v, t_0; h) = \frac{1}{Bh} \sum_{i=1}^B \phi\left(\frac{v - v_i^*(t_0)}{h}\right), \tag{C-1}$$

where $\phi(x)$ is the normal probability density function, $(1/\sqrt{2\pi}) \times \exp(-x^2/2)$. The parameter h is the window size of the

Gaussian density kernel estimator and regulates the amount of smoothing of the density estimate. The smoothing is computed using the following expression (Silverman, 1986):

$$h = 1.06\sigma^* B^{-0.2}, \tag{C-2}$$

where σ^* is an estimate of the standard error of v_i^* , $i = 1, B$. Equation (C-1) is interpreted as adding up B small Gaussian curves centered around v_b^* , each having standard error h . Larger values of h will produce a smoother density estimate.